Accuracy of Evaluation of Fatty Liver with Third-Generation Unenhanced Dual-Energy CT and MRI: Prospective Comparison with MR Spectroscopy

S. Rajesh[1]   Venkatesh Kasi Arunachalam[1]   Gopinath Periaswamy[1]   Gobi Kalyan[1]
Rupa Renganathan[1]   Gowtham S.M.[1]   Mathew Cherian[1]

[1] Department of Radiology, Kovai Medical Center and Hospital, Coimbatore, Tamil Nadu, India

J Gastrointestinal Abdominal Radiol ISGAR 2023;6:79–88.

Address for correspondence Venkatesh Kasi Arunachalam, DMRD, DNB, FRCR, Department of Radiology, Kovai Medical Center and Hospital (KMCH), Avanashi Road, Coimbatore 641014, Tamil Nadu, India (e-mail: drkasivenkatesh@yahoo.co.in).

Abstract

Background and Objectives   The purpose of this study is to evaluate and establish the accuracy of noninvasive methods, including third-generation dual-source dual-energy computed tomography (DECT) and proton density fat (PDF) fraction on magnetic resonance imaging (MRI) using three-dimensional multiecho multipoint chemical shift-encoded spoiled gradient echo (q-Dixon) sequence in the quantification of hepatic steatosis; with H1-MR spectroscopy (MRS) as the reference standard.

Materials and Methods   A total of 47 patients were included in this prospective study. We studied the accuracy of fatty liver detection using third-generation DECT using mixed set images (MSIs), virtual monochromatic images (VMIs), and MRI q-Dixon. The results were compared with H1-MRS. Data were analyzed using linear regression for each technique compared with MRS.

Results   Our study's correlation and linear regression analysis showed a good correlation between PDF values obtained by H1-MRS and MR q-Dixon methods ($r = 0.821$, $r^2 = 0.674$, $p < 0.001$). On MSI, H1-MRS showed a low correlation with average liver attenuation ($r^2 = 0.379$, $p < 0.001$) and a moderate correlation with liver attenuation index ($r^2 = 0.508$, $p < 0.001$) noted. There was a moderate correlation between H1-MRS and average liver attenuation and liver attenuation index on VMI at 80 to 120 keV with $r^2 = 0.434$, $p < 0.001$, and $r^2 = 0.485$, $p < 0.001$, respectively.

Conclusion   MRI q-Dixon is the method of choice for evaluating fat quantification in the absence of H1 MRS. Among DECT images, VMI is valuable in the evaluation of hepatic fat as compared with the mixed set of images.

Keywords
► virtual monochromatic
► third generation
► dual-source
► dual-energy
► PDFF
► q-Dixon
► fat quantification
► noncontrast

Introduction

Various population studies have shown that at least 30% of the general adult population in India has fatty liver.[1,2] A liver is considered "fatty" or "steatotic" when the total fat content exceeds 5% of the wet weight of the liver.[3,4] The imaging modalities which can detect and quantify the hepatic fat content noninvasively include ultrasound (USG), unenhanced computed tomography (CT), and magnetic resonance imaging (MRI)-based methods (chemical shift MRI and proton MR spectroscopy [MRS]).[5] Only a few studies have evaluated the role of dual-energy CT (DECT) in quantifying hepatic fat. Our study aimed to evaluate the accuracy of unenhanced scan acquired using third-generation DECT, and proton density fat fraction (PDFF) using multiecho three-dimensional (3D) Dixon sequence in

quantification hepatic steatosis; with H1-MRS as the reference standard.

Materials and Methods

This study had been approved by the local ethical and scientific committee, and written informed consent was obtained from all participants. All patients who were refereed by the hepatologists to rule out fatty liver to the department of radiology in our hospital were evaluated in this study. The patients who gave consent and underwent both modalities were included in this study. We prospectively studied 47 consecutive subjects in our study.

The patients were advised to come to the radiology department after midnight starvation. Immediately after the completion of MRI examination, unenhanced DECT was performed. All the examinations were performed within a period of 4 hours, usually between 8.00 a.m. to 12.00 p.m. to reduce diurnal variation. CT examinations were performed on a dual-source DECT SOMATOM Force (Siemens, Healthineers, Germany). Dual-energy unenhanced scans were acquired using the following parameters: Pitch: 0.6, field of view: 512, tube A: 100 kVp, and tube B: 150 kVp. CT images were analyzed on the syngo.via workstation (Siemens, Germany). Average liver attenuation was calculated by manually placing the circular regions of interest (ROIs) of at least 1 cm^2 area at 12 places in the liver, covering all the hepatic segments and avoiding major vessels, ducts, and fissures. Average splenic attenuation was measured by placing ROIs at its upper, mid, and lower poles. The liver attenuation index (LAI) was calculated as: average hepatic attenuation – average splenic attenuation. Average attenuation of liver (Lavg) and LAI on a mixed and monochromatic set of images (at 80, 90, 100, 110, 120 keV) were calculated from the unenhanced DECT scan.

MRI was performed on a MAGNETOM Skyra 3.0T MRI system (Siemens Healthcare, Erlangen, Germany) using a specialized application package called "LIVER LABORATORY." It includes:

T1 VIBE q-Dixon (Multiecho Multipoint Spoiled Gradient-Echo Dixon)

It is a 3D multiecho multipoint chemical shift encoded spoiled gradient-echo-based sequence. Images were routinely acquired in a single breath-hold. The multifat peak model was used for robust lipid estimation. The q-Dixon provides mean fat signal fraction values for the entire liver volume. The final report sheet was created by automated processing, and the PDFF was expressed as text and color bar. The final report had information about both fat and iron content in the liver. None of our patient had iron deposition in the liver.

HISTO (Proton MR Spectroscopy)

The HISTO was a 15-second single breath-hold, stimulated echo acquisition mode spectroscopy sequence. It used single-voxel spectroscopy, with the typical voxel size being 3 × 3 × 3 cm^3. The voxel should be positioned in liver tissue, not over vessels or the gallbladder. Reconstruction and postprocessing of HISTO-MRS were inline, creating a report sheet. The PDFF was expressed as text and color bar.

PDFF is obtained directly from the multiecho multipoint gradient-echo 3D Dixon (q-Dixon) report sheet and proton MRS sequence (HISTO) report sheet. CT and MRI were reviewed by a single radiologist with more than 8 years' experience in abdominal imaging.

Statistical Analysis

All baseline demographic were described as mean ± standard deviation (SD). In addition, the CT LAI and PDFF s obtained from the multiecho 3D Dixon and proton MRS (HISTO) were expressed as mean ± SD. Correlation and simple linear regression analysis were performed to correlate and calibrate the hepatic fat content obtained from CT and MRI against H1-MRS PDF. In addition, further Bland–Altman analysis was performed to find out the agreement between hepatic fat content obtained by each modality and H1-MRS PDF. The statistical analyses were performed with SPSS software (version 22) (SPSS, Chicago, Illinois, United States) and MedCalc 9.3 (MedCalc Software, Mariakerke, Belgium).

Results

In our study, 47 subjects who have completed all examinations without any adverse events were included. The mean age of the study population was 50.87 with SD of 14.12 years (range 20–80 years). The study population comprised of 49% males and 51% females. The mean height of the study population was 169.51 cm with SD of 5.804 cm (range 155–183 cm). The mean weight of the study population was 69.3 kg with SD of 9.9 kg (range 53–95 kg). The assessed MRI and CT parameters were as follows.

H^1-MR Spectroscopy Proton Density Fat Fraction

Frequency Distribution
The PDFF values for the study population obtained by H1-MRS (►Fig. 1) ranged from a minimum of 0.30% to maximum of 45.70% (mean 13.0%, median 11.2%, and SD 10.4%). ►Table 1 shows steatosis distribution in our study population.

MRI q-Dixon Proton Density Fat Fraction

Frequency Distribution
The PDFF values for 47 subjects in the study population obtained by MRI q-Dixon (multiecho chemical shift imaging) ranged from a minimum of 2.20% to a maximum of 30.30% (mean 11.63%, median 10.3%, and SD 7.74%).

Correlation Analysis
A strong positive correlation was noted between PDFF values obtained by H1-MRS and MR q-Dixon methods with Pearson's correlation coefficient "r" being 0.821 and p-value being < 0.001 (statistically significant).
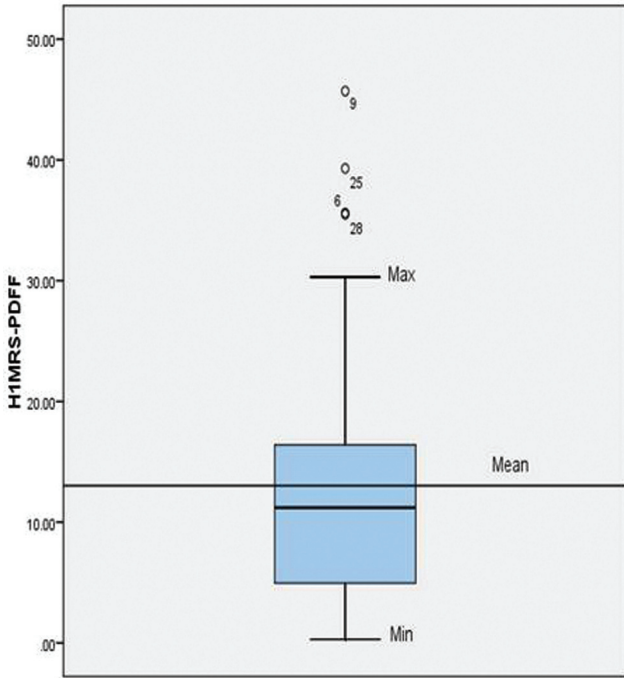
Fig. 1 Box-plot diagram showing distribution of H1-magnetic resonance spectroscopy (MRS) proton density fat fraction (PDFF) data.

Fig. 2 Graph showing results of linear regression analysis between H1-magnetic resonance spectroscopy (H1-MRS) and magnetic resonance imaging (MRI) q-Dixon proton density fat fraction (PDFF).

Linear Regression Analysis

Correlation between PDFF values obtained by H1-MRS and MR q-Dixon methods in terms of linear regression was good with coefficient of determination (r^2) being 0.674 (p-value < 0.001, statistically significant). The intercept of the regression line was 0.143 and slope was 1.107, p-value for both being < 0.001 (statistically significant) (►Fig. 2).

DECT Mixed Set Average Liver Attenuation

Frequency Distribution

The average liver attenuation values for the study population obtained by mixed set DECT ranged from a minimum of 16.0 HU to a maximum of 70.0 HU (mean 49.17 HU, median 50.0 HU, and SD 11.8 HU) (►Fig. 3).
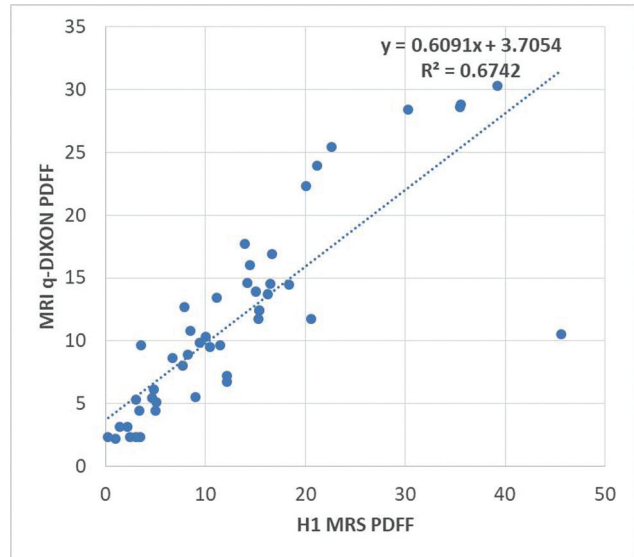
Correlation Analysis

A good negative correlation was found between PDFF values obtained by H1-MRS and average liver attenuation on unenhanced CT with Pearson's correlation coefficient "r" being -0.616 and p-value being < 0.001 (statistically significant).

Fig. 3 Box-plot diagram showing distribution of mixed dual-energy computed tomography (DECT) average attenuation of liver (Lavg) data.

Regression Analysis

Correlation between PDFF values obtained by H1-MRS and average liver attenuation values on mixed set DECT in terms of linear regression was low with coefficient of determination

Table 1 Steatosis distribution in study population

Grades of fatty liver	H1-MRS PDFF Cutoff (%)	Frequency	Percentage%
Normal	< 5.56	13	27.70
Grade I (mild)	≥ 5.56 and < 10	8	17
Grade II (moderate)	≥ 10 and < 20	17	36.2
Grade III (severe)	≥ 20	9	19.1
Total	——	47	100

Abbreviations: H1-MRS, H1-magnetic resonance spectroscopy; PDFF, proton density fat fraction.

Fig. 4 Graph showing results of linear regression analysis between H1-magnetic resonance spectroscopy (H1-MRS) and dual-energy computed tomography (DECT) average attenuation of liver (Lavg) attenuation.

(r^2) being 0.379 (p-value < 0.01, statistically significant). The intercept of the graph was 39.7 (standard error 0.995) and slope was –0.543, p-value for both being < 0.001 (statistically significant) (►**Fig. 4**).

DECT Mixed Set Liver Attenuation Index

Frequency Distribution
The CT LAI values for the study population obtained by mixed set DECT ranged from a minimum of –42.00 HU to a maxi-

mum of 18.00 HU (mean –1.78 HU, median –2.50 HU, and SD 13.7 HU).

Correlation Analysis
A good negative correlation was found between PDFF values obtained by H1-MRS and LAI on unenhanced CT with Pearson's correlation coefficient "r" being –0.713 and p-value being < 0.001 (statistically significant).
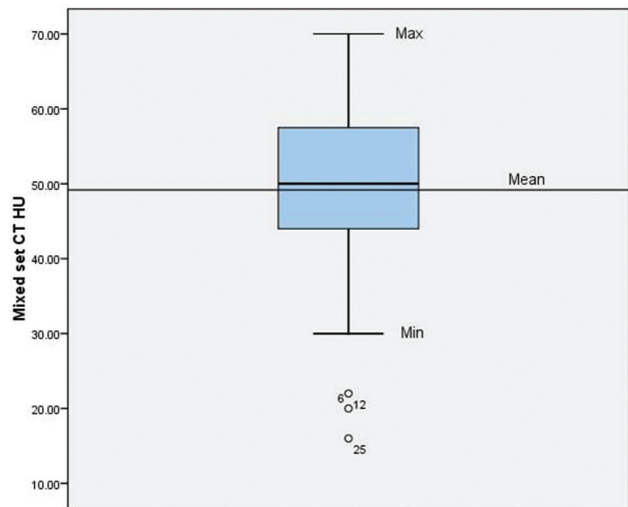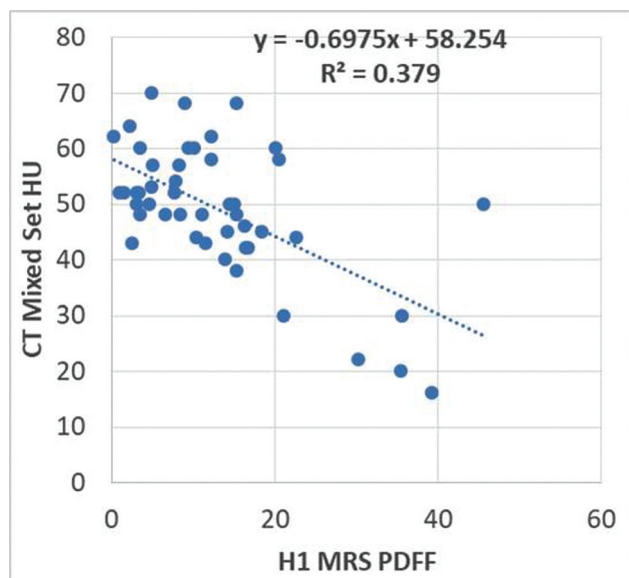
Regression Analysis
Correlation between PDFF values obtained by H1-MRS and LAI on unenhanced CT in terms of linear regression was moderate with coefficient of determination (r^2) being 0.508 (p-value 0.001, statistically significant). The intercept of the graph was 12.309 and slope was –0.541, p-value for both being < 0.001 (statistically significant) (►**Fig. 5**).

Comparison of H1-MRS MRI and Monochromatic DECT Images (80 to 120 keV)

Average Liver Attenuation
A moderate negative correlation was found between PDFF values obtained by H1-MRS and LAI on both mixed set and monochromatic DECT images with Pearson's correlation coefficient "r" between –0.57 and –0.58 (►**Table 2**).

Correlation between PDFF values obtained by H1-MRS and LAI on unenhanced both mixed set and monochromatic DECT images in terms of linear regression was moderate with coefficient of determination (r^2) being 0.43 to 0.44.
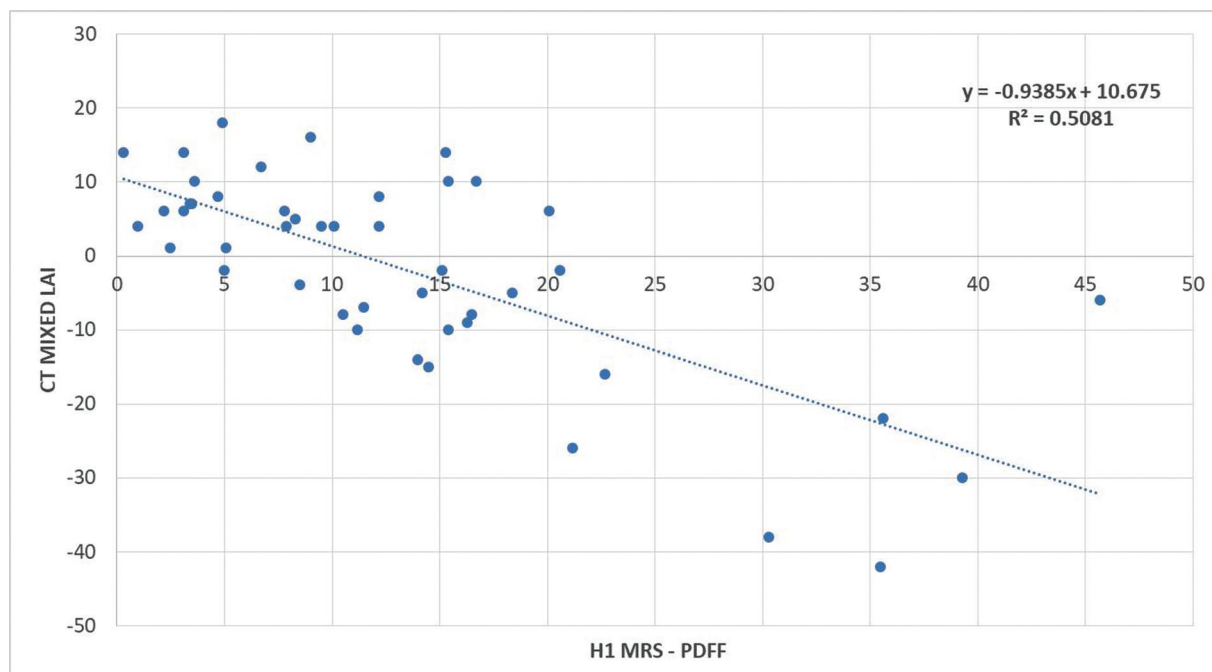
CT Liver Attenuation Index
A good negative correlation was found between PDFF values obtained by H1-MRS and LAI on both mixed set and

Fig. 5 Graph showing results of linear regression analysis between H1-magnetic resonance spectroscopy (H1-MRS) and mixed set dual-energy computed tomography (DECT) liver attenuation index (LAI).

Table 2 Results of linear regression analysis between H1-MRS and DECT Lavg attenuation—80, 90, 100, 110, and 120 keV

Lavg	80	90	100	110	120
Intercept	−0.57	−0.58	−0.57	−0.58	−0.58
Slope	41.71	42.12	41.78	42.41	42.07
R^2	0.44	0.46	0.44	0.44	0.43
Min	1.64	0.40	0.51	0.56	0.51
Max	32.55	32.85	32.03	31.95	32.26

Abbreviations: DECT, dual-energy computed tomography; H1-MRS, H1-magnetic resonance spectroscopy; Lavg, average attenuation of liver.

Table 3 Results of linear regression analysis between H1-MRS and DECT LAI attenuation—80, 90, 100, 110, and 120 keV

LAI	80	90	100	110	120
Intercept	11.45	11.52	11.47	11.68	11.57
Slope	−0.62	−0.62	−0.63	−0.64	−0.63
R^2	0.55	0.58	0.57	0.57	0.56
Min	0.38	−0.96	−1.16	−1.05	−1.05
Max	36.05	35.25	33.56	34.60	34.30

Abbreviations: DECT, dual-energy computed tomography; H1-MRS, H1-magnetic resonance spectroscopy; LAI, liver attenuation index.

Table 4 Diagnostic performance of different imaging methods for diagnosis of all grades of hepatic steatosis with H1-MRS PDFF

H1-MRS PDFF	MRI q-Dixon PDFF	Mixed set CT Lavg HU	Mixed set CT LAI	DECT LAI (80–120 keV)	DECT LAI Lavg 80–120 keV
Sensitivity	97.0%	72.7%	63.6%	60.6%	66.7%
Specificity	85.7%	50.0%	92.9%	78.6%	92.9%
Positive predictive value	94.1%	77.4%	95.5%	87.0%	95.7%
Negative predictive value	92.3%	43.8%	52.0%	45.8%	54.2%
Accuracy	93.6%	66.0%	72.3%	66.0%	74.5%

Abbreviations: CT, computed tomography; DECT, dual-energy computed tomography; H1-MRS, H1-magnetic resonance spectroscopy; LAI, liver attenuation index; Lavg, average attenuation of liver; MRI, magnetic resonance imaging; PDFF, proton density fat fraction.

monochromatic DECT images with Pearson's correlation coefficient "r" being between −0.63 and −0.64, respectively (►**Table 3**).

Correlation between PDFF values obtained by H1-MRS and LAI on unenhanced both mixed set and monochromatic

DECT images in terms of linear regression was moderate with coefficient of determination (r^2) being between 0.55 and 0.58.

Comparison of Diagnostic Performance of Different Imaging Methods for Hepatic Fat Quantification

The diagnostic performances of various imaging modalities for diagnosis of all grades of hepatic steatosis are summarized in ►**Table 4**. The areas under curve for diagnosis of all grades of hepatic steatosis obtained by receiver operating characteristic curve analysis for different imaging methods were compared using the DeLong test to find the statistical significance of the difference (►**Table 5**).

Table 5 Comparison of AUCs of different imaging methods for diagnosis of all grades of hepatic steatosis

Test result variable(s)	AUC
MRI q-DIXON PDFF	0.982
Mixed set DECT Lavg HU	0.290
Mixed set DECT LAI	0.195
DECT Lavg at 80–120 keV	0.244
DECT LAI at 80–120 keV	0.160

Abbreviations: AUC, area under the curve; DECT, dual-energy computed tomography; LAI, liver attenuation index; Lavg, average attenuation of liver; MRI, magnetic resonance imaging; PDFF, proton density fat fraction.

Discussion

The fatty liver disease spectrum consists of simple fatty liver to steatohepatitis and cirrhosis. Liver biopsy is considered the gold standard of diagnosis and severity assessment of fatty liver, but generally, it is not accepted by patients

because it is an invasive procedure. Instead, noninvasive methods such as USG, CT, and MRI, have been used widely in diagnosing fatty liver because of their relatively high sensitivity and repeatability. Till now, only a few studies[5–7] have been reported in the literature, which has simultaneously compared the diagnostic accuracy of all three evaluated imaging modalities (MRI, DECT, and USG) for fat quantification. Since the Dallas Heart Study results were published by Szczepaniak et al[8] in 2005, H1-MRS has often been used as the reference standard for liver fat quantification in diagnostic studies and as a clinical endpoint in observational studies and clinical trials.

Our study aimed to find the correlation between hepatic fat fractions obtained by advanced imaging methods and the reference standard PDFF obtained by H1-MRS using correlation and linear regression models. We used receiver operating curve analysis to determine the area under the curve for diagnosing hepatic steatosis using all methods and derived

corresponding cutoffs adjusting optimal sensitivity and specificity. Finally, we compared the areas under the curve using the DeLong[9] test to determine which method had a better diagnostic performance.

We calculated the distribution of hepatic steatosis in our study population based on the cutoff values of H1-MRS PDF (13, 59)—5.56% between no and mild steatosis, 10% between mild and moderate, and 20% between moderate and severe steatosis. Accordingly, in our study, 27.7% had no steatosis (►**Fig. 6**), 17% had grade I - mild steatosis, 36.2% had grade II - moderate steatosis (►**Fig. 7**), and 19.1% were diagnosed with grade III - severe steatosis (►**Figs. 8** and **9**).

Correlation between H1-MRS and MR q-Dixon
The correlation and linear regression analysis results in 47 subjects showed a good correlation between PDF values obtained by H1-MRS and MR q-Dixon methods ($r = 0.821$, $r^2 = 0.674$, $p < 0.001$). The results of this study are
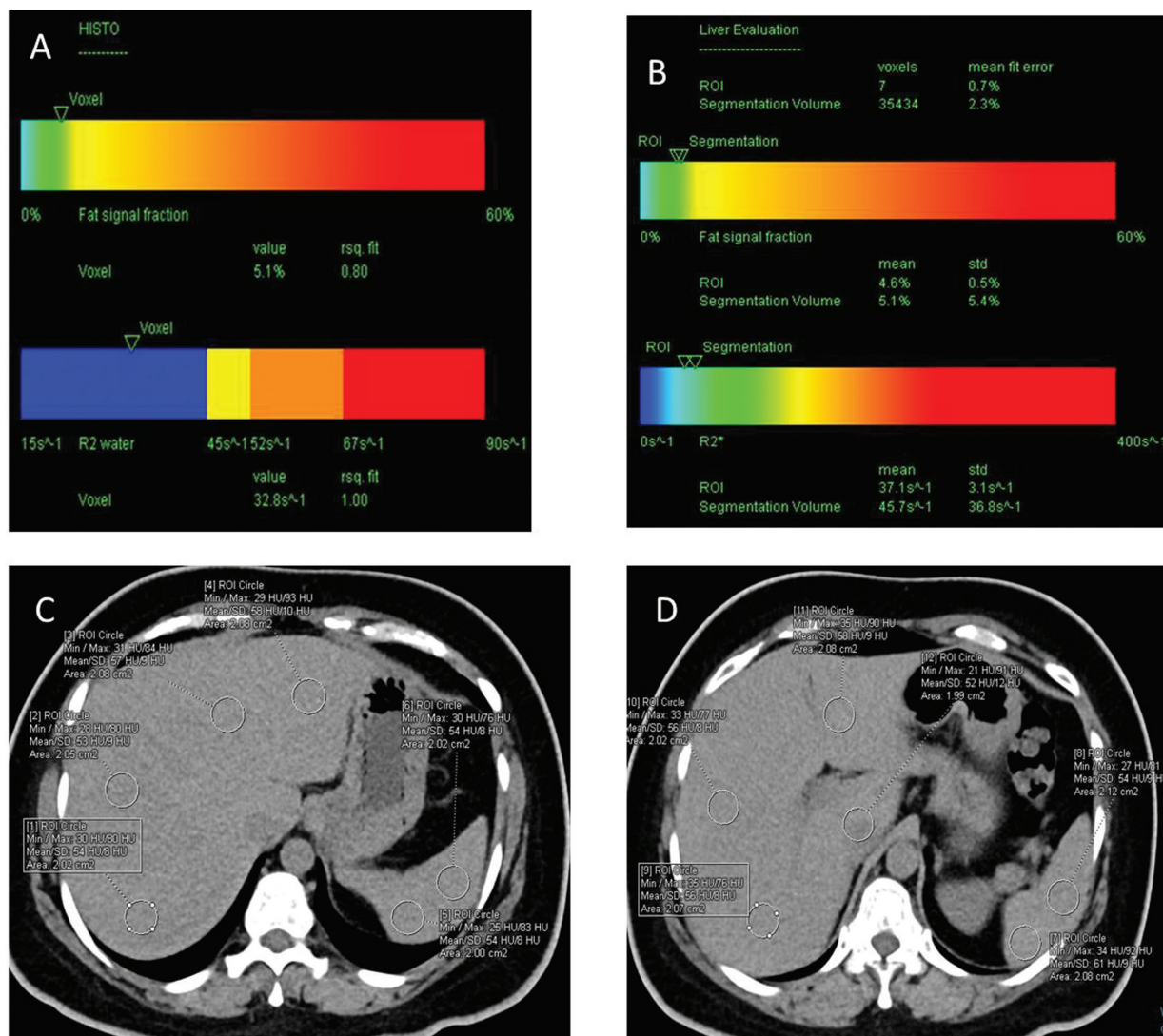
Fig. 6 A 38-year-old female patient with no fatty liver. H1-magnetic resonance spectroscopy (H1 MRS0 (HISTO) showing proton density fat fraction (PDFF) of 5.1% (**A**). MR q-Dixon report sheet (**B**) of the same patient showing PDFF of 5.1%. Unenhanced dual-energy computed tomography (DECT) mixed set of images (**C**, **D**) of the same patient with region of interest (ROI) drawn at all segments of liver and spleen. Average liver attenuation value is 55 and liver attenuation index (average liver attenuation – average spleen attenuation) is 0.
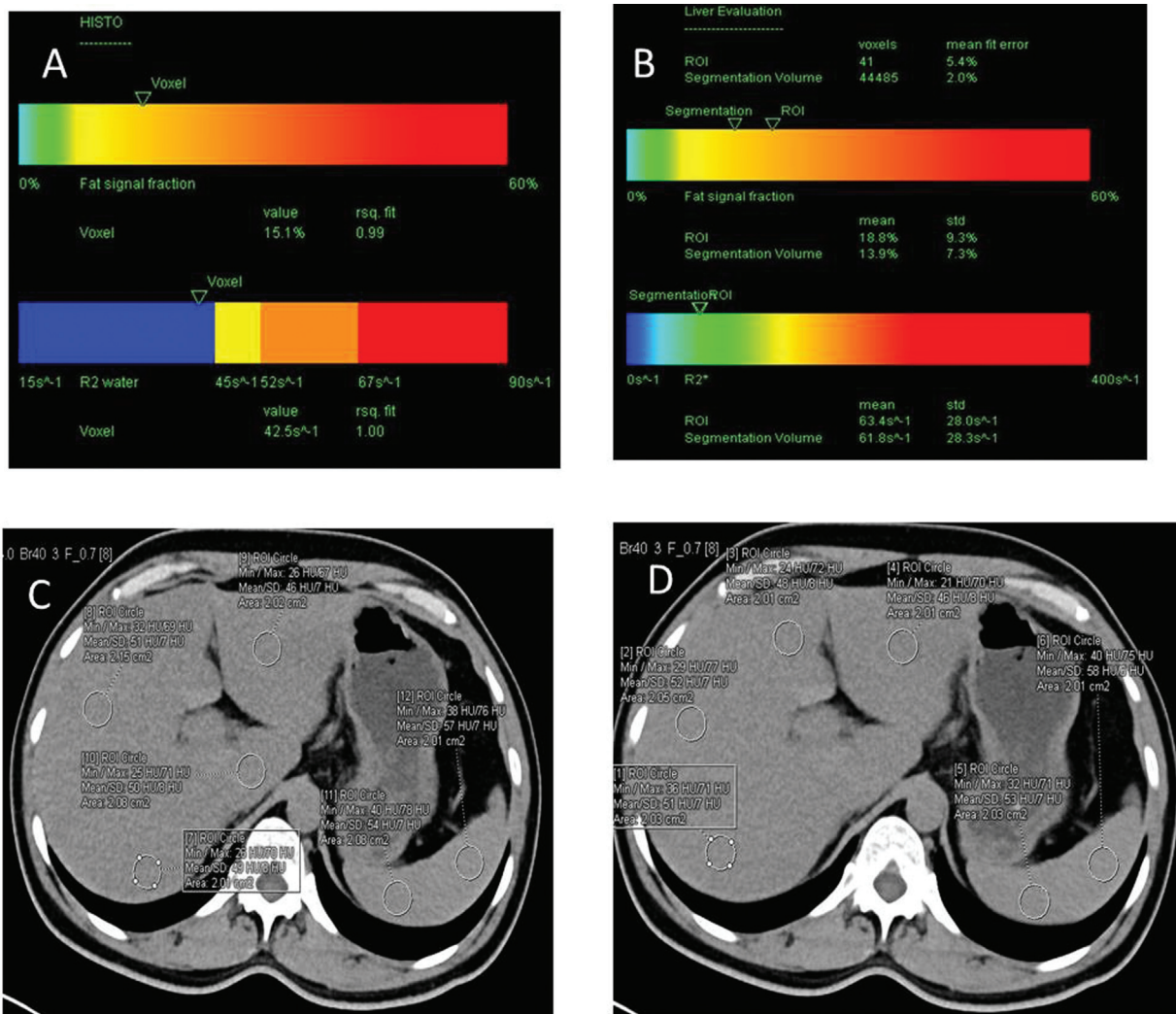
Fig. 7 A 41-year-old male patient with moderate fatty liver. H1-magnetic resonance spectroscopy (H1 MRS) (HISTO) showing proton density fat fraction (PDFF) of 15.1% (**A**). MR q-Dixon report sheet (**B**) of the same patient showing PDFF of 13.9%. Unenhanced dual-energy computed tomography (DECT) mixed set of images (**C**, **D**) with region of interest (ROI) drawn at all segments of liver and spleen. Average liver attenuation value is 49.5 and liver attenuation index (average liver attenuation – average spleen attenuation) is –6.

comparable to those of a previous study done by Kramer et al.[5] They showed excellent correlation ($r^2 = 0.992$, $p < 0.001$) between PDF values obtained by H1-MRS and an investigational multiecho 3D spoiled gradient-echo chemical shift technique. Based on receiver operating curve analysis, we derived an optimal cutoff value of 5.5% for diagnosing hepatic steatosis and 8.8% for diagnosing moderate to severe hepatic steatosis by MR q-Dixon method in this study. The area under the curve was 0.923. The sensitivity, specificity, and accuracy at this cutoff value were 97, 86, and 97%. Ishizaka et al[10] also had found similar results with multiecho gradient-echo chemical shift technique showing the specificity of 98% for the diagnosis of all grades of hepatic steatosis.

### Correlation between H1-MRS and Unenhanced DECT Mixed Set Images

On CT, we studied the accuracy of fatty liver detection in mixed set and virtual monochromatic images at 80 to 120 keV generated using third-generation dual-source DECT. We used two methods to quantify hepatic steatosis using unenhanced CT: (1) average liver attenuation and (2) CT LAI.

Average Liver Attenuation

The Lavg on unenhanced CT scan showed moderate negative correlation ($r = -0.616$, $p < 0.001$) with H1-MRS PDF. Linear regression showed a low correlation between the two methods with $r^2 = 0.379$, $p < 0.001$. However, in the study conducted by Kramer et al,[5] an excellent correlation was found between mean attenuation of liver and H1-MRS PDFF with $r^2 = 0.860$. The difference in the results may be explained by scanner-related and patient population-related differences in attenuation values obtained on unenhanced CT.

Receiver operating curve analysis revealed an area under the curve of 0.290 for diagnosis of all grades of steatosis using CT-derived average liver attenuation values. We further derived an optimal cutoff of 54 HU for diagnosing all grades of hepatic steatosis, and for diagnosing moderate to severe hepatic steatosis, we found a cutoff value of 47 HU. The sensitivity, specificity, and accuracy for grading of hepatic
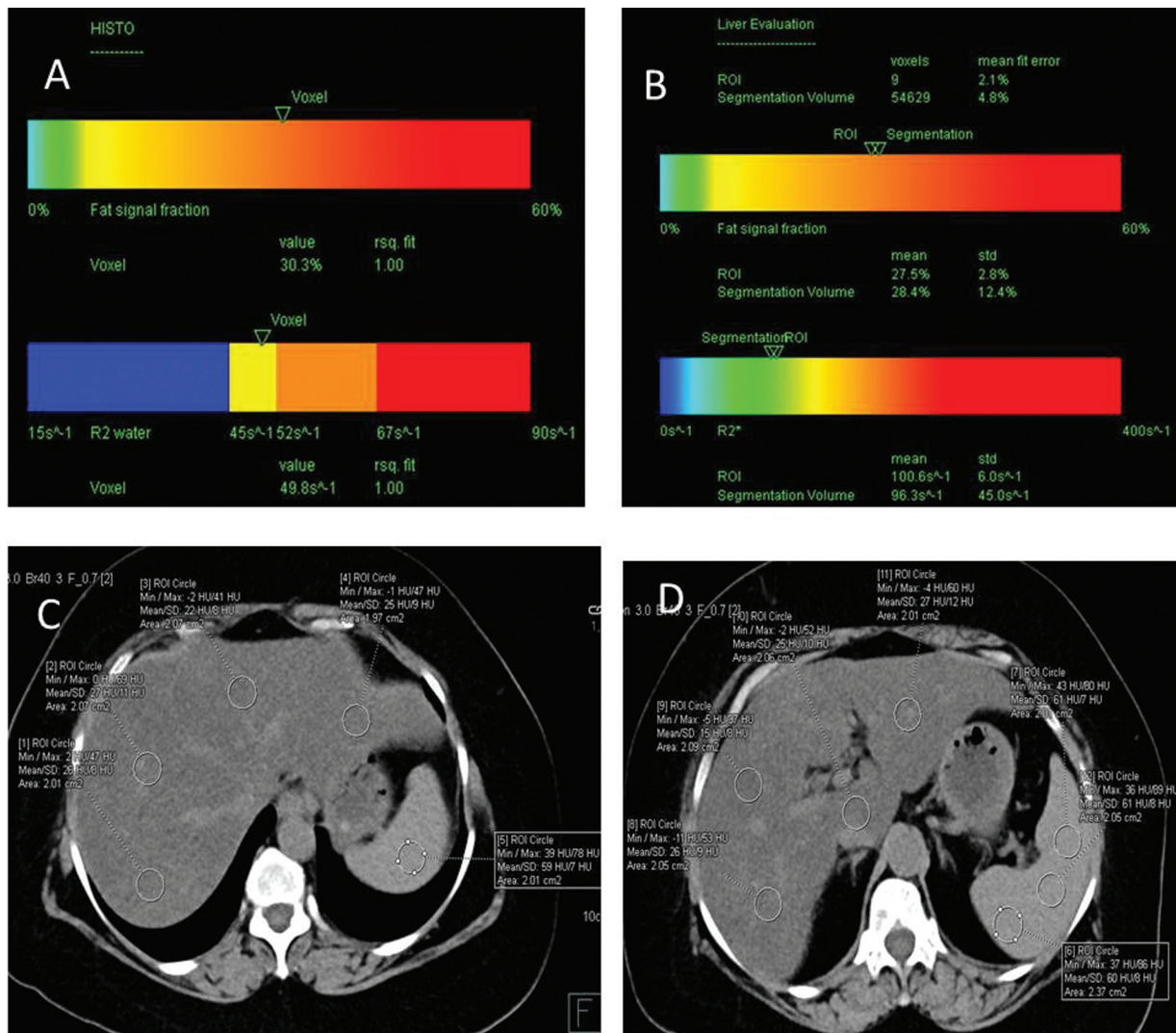
Fig. 8 A 53-year-old female patient with severe fatty liver. H1-magnetic resonance spectroscopy (H1 MRS) (HISTO) showing proton density fat fraction (PDFF) of 30.3%. MR q-Dixon report sheet (**B**) showing PDFF of 28.4%. Unenhanced dual-energy computed tomography (DECT) mixed set of images (**C, D**) with region of interest (ROI) drawn at all segments of liver and spleen. Average liver attenuation value is 24 and liver attenuation index (average liver attenuation – average spleen attenuation) is –36.

steatosis were 72, 50, and 66%, respectively. Different studies have proposed different cutoff values for the diagnosis of hepatic steatosis. The cutoff value of 54 HU obtained by our study for diagnosing all grades of hepatic steatosis is similar to that of 54.2 HU by van Werven et al[11] in their study. The cutoff value of 47 HU for diagnosis of moderate to severe hepatic steatosis is comparable to that of 48 HU proposed by Pickhardt et al.[12]

CT Liver Attenuation Index

The LAI on unenhanced DECT mixed set images showed moderate negative correlation, $r = -0.713$, $p < 0.001$, with H1-MRS PDF. Linear regression also showed a moderate correlation between the two methods. Our results are comparable to those obtained by Rastogi et al,[13] where they showed a moderate correlation between CT LAI and MRS PDF ($r = -0.713$).

Receiver operating curve analysis revealed an area under the curve of 0.195 for diagnosis of all grades of steatosis using

CT-based LAI values. We further derived an optimal cutoff of –1 HU for diagnosing all grades hepatic steatosis and –9 HU for diagnosing moderate to severe hepatic steatosis. The sensitivity, specificity, and accuracy were 63.6, 92.9, and 72.3%, respectively. Our cutoff value of –1 HU for diagnosing hepatic steatosis is comparable to that of 1 HU proposed by Park et al.[14] The cutoff value of –9 HU for moderate to severe steatosis is similar to that of –9 HU derived by Park et al.[15]

Correlation between H1 MRS MRI and Monochromatic

DECT Images (80, 90, 100, 110, and 120 keV)

Average Liver Attenuation

The Lavg on unenhanced CT scan showed moderate negative correlation ($r = -0.659$, $p < 0.001$) with H1-MRS PDFF. Linear regression also showed moderate correlation between the two methods with $r^2 = 0.434$, $p < 0.001$. It is similar to the results in a study conducted by Kramer et al,[5] moderate
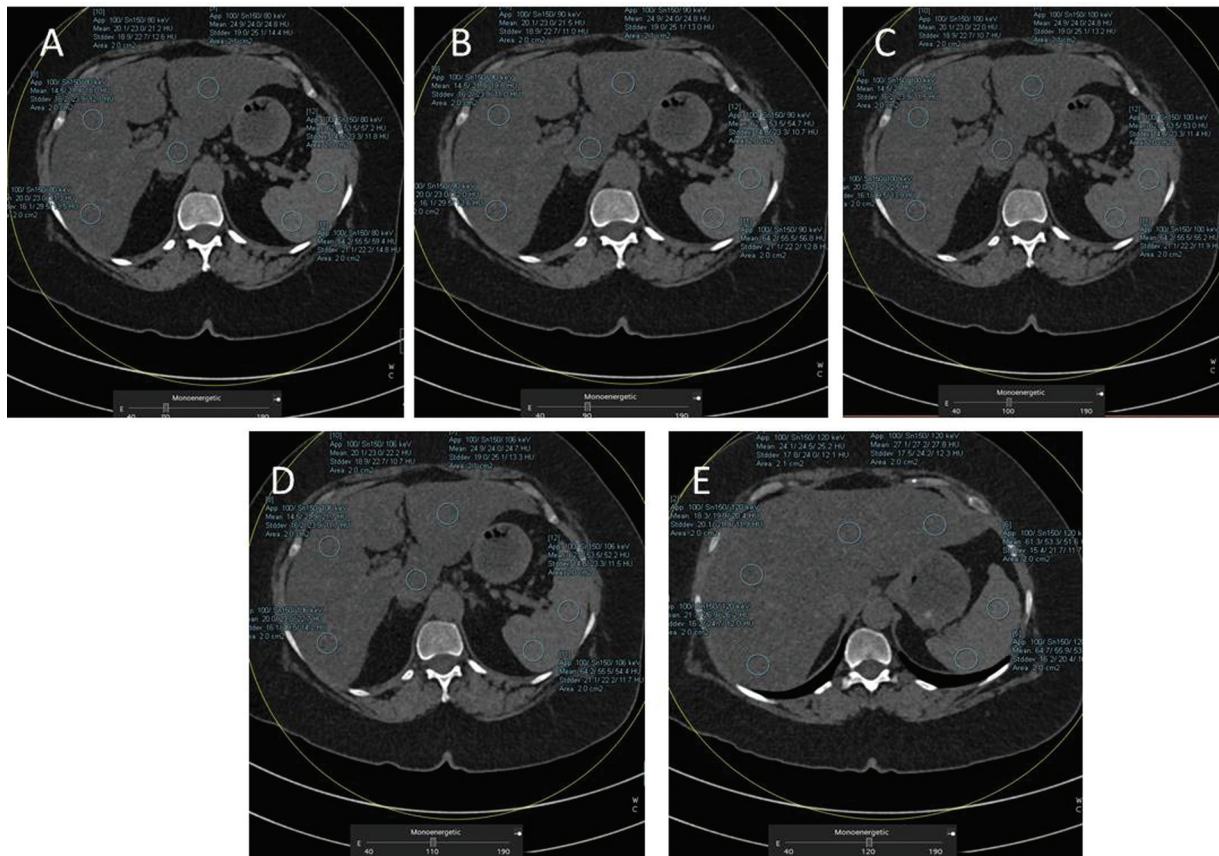
Fig. 9 A 53-year-old female patient with severe fatty liver. Unenhanced dual-energy computed tomography (DECT) virtual monochromatic images (A–E) of the same patient in ►**Fig. 8** from 80 to 120 keV levels with region of interest (ROI) drawn over liver and spleen.

correlation was found between DECT Lavg and H1-MRS PDFF with $r^2 = 0.423$.

Receiver operating curve analysis revealed an area under curve of 0.244 for diagnosis of all grades of steatosis using DECT deriving average liver attenuation values with sensitivity, specificity, and accuracy of 60.6, 78.6, and 66%, respectively.

CT Liver Attenuation Index
The LAI on unenhanced CT scan showed moderate negative correlation ($r = -0.696, p < 0.001$) with H1-MRS PDFF. Linear regression also showed moderate correlation between the two methods with $r^2 = 0.485, p < 0.001$.

Receiver operating curve analysis revealed an area under curve of 0.160 for diagnosis of all grades of steatosis using CT-based LAI values with corresponding sensitivity, specificity, and accuracy of 66, 92, and 74%, respectively.

Both methods, that is, average liver attenuation and LAI evaluated on monochromatic DECT on particular keV separately at 80, 90, 100, 110, and 120 keV did not show any statistically significant difference in correlation for evaluating fatty liver when compared with H1-MRS PDF.

One of the major limitations of CT is ionizing radiation exposure. To reduce the exposure to ionizing radiation, most CT scanners have dose modulation tools, which modify tube current within an acquisition and thus, may have different settings for every single acquired slice. In general, densities measured in CT data sets very much rely on the scanning parameters, especially tube energy.

Correlation between H1-MRS, MRI, and Unenhanced DECT (Mixed Set and Monochromatic Images)
The LAI on both mixed set and monochromatic DECT scan showed a moderate negative correlation with H1-MRS PDF. Correlation between PDF values obtained by H1-MRS and average liver attenuation on unenhanced mixed set DECT was low with $r^2 = 0.379$ and was good on monochromatic DECT image at 80 to 120 keV with $r^2 = 0.434$. For evaluating fatty liver with average liver attenuation, monochromatic DECT image at 80 to 120 keV correlates better than mixed set images with H1-MRS.

Comparison of MRI, Unenhanced DECT, and USG Methods
The current study compared unenhanced DECT and MRI q-Dixon and found that quantitative MRI q-Dixon PDFF shows a good correlation with H1-MRS-derived PDFF measurements. Unenhanced DECT-based methods LAI and Lavg (mixed set and monochromatic) showed moderate correlation (except Lavg on mixed set images which showed low correlation). The comparison of area under curve revealed that MRI q-Dixon method performed the best for diagnosis of all grades

of hepatic steatosis compared with the rest. The difference in the areas under the curve of MRI q-Dixon with other methods was statistically significant ($p < 0.05$ for all comparisons). The findings of our study were similar to that of Lee et al[16] and van Werven et al.[11] They also had reported that chemical shift MRI performed better than CT for diagnosis of hepatic steatosis. The meta-analysis by Bohte et al[6] had also revealed that MRI methods perform better than USG and CT for detecting separate disease grades, especially for mild disease ($< 30\%$ steatosis on histology).

There were a few limitations to our study. First, H1-MRS was used as the reference standard without histopathologic correlation. However, similar to tissue biopsy, the spatially heterogeneous distribution of hepatic fat is also a confounding factor that limits the use of H1-MRS as a reference standard. Second, we used a dual-source DECT scanner for evaluating the fatty liver, which may not be reproducible in other vendors' specific CTs. Further studies with different DECT techniques/vendors are needed. Third, few pathological states like hemochromatosis and glycogenosis may result in an abnormal alteration of liver density and affect the CT attenuation value measurement accuracy, masking the underlying fatty liver. This aspect was not evaluated in our study.

Conclusion

3D multiecho multipoint chemical shift-encoded spoiled gradient echo (q-Dixon) sequence shows a good correlation with H1-MRS in hepatic fat quantification. Adding this sequence to the normal standard-of-care liver or abdominal MRI examination will minimally lengthen the examination duration; however, it benefits quantifying liver fat content over the entire organ. In DECT, virtual monochromatic DECT is better for evaluating fatty liver with average liver attenuation than mixed set images. There is no significant difference in correlation for assessing fatty liver with LAI and average liver attenuation using virtual monochromatic DECT images among particular keV at 80, 90, 100, 100, 110, and 120 keV compared with H1-MRS. So, it will not add much diagnostic value to reconstruct a particular keV for evaluating fatty liver. Although unenhanced DECT using virtual monochromatic images and mixed set images shows limited diagnostic performance than MRI, it can be used in diagnosing steatosis while evaluating other abdominal pathologies or screening abdomen and in preoperative liver donor evaluation.

Conflict of Interest
None declared.

References

1 Amarapurkar D, Kamani P, Patel N, et al. Prevalence of non-alcoholic fatty liver disease: population based study. Ann Hepatol 2007;6(03):161–163

2 Mohan V, Farooq S, Deepa M, Ravikumar R, Pitchumoni CS. Prevalence of non-alcoholic fatty liver disease in urban south Indians in relation to different grades of glucose intolerance and metabolic syndrome. Diabetes Res Clin Pract 2009;84(01):84–91

3 Ratziu V, Bellentani S, Cortez-Pinto H, Day C, Marchesini G. A position statement on NAFLD/NASH based on the EASL 2009 special conference. J Hepatol 2010;53(02):372–384

4 Veteläinen R, van Vliet A, Gouma DJ, van Gulik TM. Steatosis as a risk factor in liver surgery. Ann Surg 2007;245(01):20–30

5 Kramer H, Pickhardt PJ, Kliewer MA, et al. Accuracy of liver fat quantification with advanced CT, MRI, and ultrasound techniques: prospective comparison with MR spectroscopy. AJR Am J Roentgenol 2017;208(01):92–100

6 Bohte AE, van Werven JR, Bipat S, Stoker J. The diagnostic accuracy of US, CT, MRI and 1H-MRS for the evaluation of hepatic steatosis compared with liver biopsy: a meta-analysis. Eur Radiol 2011;21(01):87–97

7 Lee SS, Park SH. Radiologic evaluation of nonalcoholic fatty liver disease. World J Gastroenterol 2014;20(23):7392–7402

8 Szczepaniak LS, Nurenberg P, Leonard D, et al. Magnetic resonance spectroscopy to measure hepatic triglyceride content: prevalence of hepatic steatosis in the general population. Am J Physiol Endocrinol Metab 2005;288(02):E462–E468

9 DeLong ER, DeLong DM, Clarke-Pearson DL. Comparing the areas under two or more correlated receiver operating characteristic curves: a nonparametric approach. Biometrics 1988;44(03):837–845

10 Ishizaka K, Oyama N, Mito S, et al. Comparison of 1H MR spectroscopy, 3-point DIXON, and multi-echo gradient echo for measuring hepatic fat fraction. Magn Reson Med Sci 2011;10(01):41–48

11 van Werven JR, Marsman HA, Nederveen AJ, et al. Assessment of hepatic steatosis in patients undergoing liver resection: comparison of US, CT, T1-weighted dual-echo MR imaging, and point-resolved 1H MR spectroscopy. Radiology 2010;256(01):159–168

12 Pickhardt PJ, Park SH, Hahn L, Lee S-G, Bae KT, Yu ES. Specificity of unenhanced CT for non-invasive diagnosis of hepatic steatosis: implications for the investigation of the natural history of incidental steatosis. Eur Radiol 2012;22(05):1075–1082

13 Rastogi R, Gupta S, Garg B, Vohra S, Wadhawan M, Rastogi H. Comparative accuracy of CT, dual-echo MRI and MR spectroscopy for preoperative liver fat quantification in living related liver donors. Indian J Radiol Imaging 2016;26(01):5–14

14 Park YS, Park SH, Lee SS, et al. Biopsy-proven nonsteatotic liver in adults: estimation of reference range for difference in attenuation between the liver and the spleen at nonenhanced CT. Radiology 2011;258(03):760–766

15 Park SH, Kim PN, Kim KW, et al. Macrovesicular hepatic steatosis in living liver donors: use of CT for quantitative and qualitative assessment. Radiology 2006;239(01):105–112

16 Lee SS, Park SH, Kim HJ, et al. Non-invasive assessment of hepatic steatosis: prospective comparison of the accuracy of imaging examinations. J Hepatol 2010;52(04):579–585